

# Learning Behavioral Representations of Human Mobility <sup>\*</sup>

Maria Luisa Damiani

maria.damiani@unimi.it

Andrea Acquaviva

andrea.acquaviva1@studenti.unimi.it

Fatima Hachem

fatme.hachem@unimi.it

Matteo Rossini

matteo.rossini@unimi.it

Department of Computer Science  
University of Milan, Italy

## Abstract

In this paper, we investigate the suitability of state-of-the-art representation learning methods to the analysis of behavioral similarity of moving individuals, based on CDR trajectories. The core of the contribution is a novel methodological framework, *mob2vec*, centered on the combined use of a recent symbolic trajectory segmentation method for the removal of noise, a novel trajectory generalization method incorporating behavioral information, and an unsupervised technique for the learning of vector representations from sequential data. *mob2vec* is the result of an empirical study conducted on real CDR data through an extensive experimentation. As a result, it is shown that *mob2vec* generates vector representations of CDR trajectories in low dimensional spaces which preserve the similarity of the mobility behavior of individuals.

## 1 Introduction

Core resources for the study of human mobility are the datasets of Call Detail Records (CDR) [5]. CDRs report the communication activities of mobile communication subscribers as series of geo-referenced events, i.e., voice call start/end, text message, data upload/download, collected by mobile operators for billing purposes [9]. We refer to a series of temporally ordered CDRs associated to an individual as CDR trajectory. Abstractly, CDR trajectories can be represented as sequences of timestamped symbolic locations (i.e. geo-referenced symbols), for example, base station identifiers. Therefore, given a

set of symbolic locations  $L$ , a CDR trajectory  $T$  can be represented by the sequence:

$$T = (l_1, t_1), \dots, (l_n, t_n) \quad \text{with } l_i \in L$$

CDR trajectories are complex data, encompassing both the spatio-temporal and the textual dimensions, irregularly sampled, spatially sparse, and noisy. Yet, CDR data offer unique opportunities for the study of human mobility because of the large base of users monitored in their daily life.

Seminal research on human mobility modeling has shown that people exhibit a high degree of regularity in their motion [13, 25]. In particular, individuals visit recurrently few locations and only sometimes divert from their habitual trips to visit new locations [13]. While regularity is a well established characteristic of human mobility, on which there is a broad consensus in literature, a challenging question is how to compare the mobility behavior of individuals and determine whether and to what extent those behaviors are similar. As an example, consider users  $u_1$  and  $u_2$ , and suppose that  $u_1$  travels daily from location  $l_1$  to  $l_2$  and back to  $l_1$ , thus exhibiting the pattern  $l_1 \rightarrow l_2 \rightarrow l_1$ , while user  $u_2$  follows the pattern  $l_3 \rightarrow l_4 \rightarrow l_3$ ; moreover assume that both users very rarely frequent other locations. The intuition is that the mobility behavior is similar, regardless of the actual locations where they stay, e.g., users visit a similar number of locations in a similar way. We refer to this form of similarity as *behavioral similarity*.

Behavioral similarity is hard to define. Besides, it does not depend on the specificity of locations and thus cannot be approached using classic similarity metrics, e.g. [3], sequential pattern mining techniques, e.g. [11, 19], recent techniques for the representation learning [2] of user activities graphs, e.g. [27, 28]. To tackle the problem, a viable approach is to characterize the individual behavior by measuring selected mobility features. For example, a metric widely used by the human mobility research community, is the radius of gyration  $R_g$  (and its variants, e.g. [1, 22]) measuring the distance from the trajectory

<sup>\*</sup>The final version of this work will appear in the proceedings of ACM SIGSPATIAL 2020 with DOI: 10.1145/3397536.3422255. Please refer to the final version for future citations.

center of mass. High values of  $R_g$  are interpreted as high user’s propensity to mobility. Another kind of measure is *true location diversity*, an entropy-based metric that we have recently proposed to quantify the heterogeneity of locations in symbolic trajectories [9]. In general, however, the approaches grounded on the choice of metrics present an important shortcoming, namely it is not clear which mobility features are really significant to characterize the mobility behavior. Consequently any metric results arbitrary or partial.

To deal with the question, we explore a novel approach built on representation learning, applied to generalized trajectories incorporating behavioral information. For this study, we consider CDR trajectories limited to their symbolic and temporal dimensions. The idea is to investigate the suitability of techniques drawn from NLP, i.e. word2vec [18] and Paragraph Vector [6, 15], to generate vector representation of CDR trajectories. The problem can be broadly formulated as follows: given an  $n$ -dimensional vector space  $\mathbb{R}^n$  and a dataset  $D$  of trajectories, we search for a mapping  $f: D \rightarrow \mathbb{R}^n$  capable of preserving mobility behavior similarity.  $\mathbb{R}^n$  is the *embedding space*, the vector  $v = [x_1, \dots, x_n]$  the trajectory representation or *trajectory embedding*. CDR trajectories have peculiar features which raise important challenges: the dictionary of symbols is small (a few hundred symbols), trajectories are of different length, symbols are temporally annotated, data are noisy and contain a large number of rarely frequented locations. Therefore, the representation learning techniques used in NLP cannot be straightforwardly applied to CDR trajectories. On the other hand, existing techniques for the vector representation of trajectories, such as [16, 26], focus on spatial trajectories, thus overlooking the discrete, symbolic dimension of movement, while, by contrast, techniques focusing on symbolic locations typically organize the set of locations visited by users in graphs, and not in temporal sequences, e.g [4, 27], or rather interpret behavioral similarity in terms of location similarity, e.g. [29].

In this paper, we present an empirical approach to the generation of trajectory embeddings resulting in a methodological framework called *mob2vec*. *mob2vec* is the outcome of an extensive experimentation conducted for evaluating different options and alternative directions. *mob2vec* is grounded on a number of key design choices, in particular:

- It builds on a state-of-the-art technique for the generation of embeddings for symbolic sequences called Sqn2Vec [20]. Sqn2Vec is grounded on a feedforward Neural Network architecture and can be applied to datasets of sequences of arbitrary length and containing a limited number of symbols. This technique, however, does not provide any support to deal with time and noisy data.

- It leverages a technique we have recently proposed for the removal of noise and extraction of significant locations from CDR and symbolic trajectories, called SeqScan-d. The resulting trajectories are called *summary trajectories* [9].
- Summary trajectories are mapped onto generalized trajectories in which location names are replaced by a measure of location relevance, expressed in terms of *frequency rank*. For example, the most visited location has rank 1, the second most visited rank 2 and so on. The rank variable thus takes ordinal values. The resulting trajectories are called *rank trajectories*.

These design choices drive the representation learning process, which consists of the following steps: *data preparation* turns CDR trajectories into noise-free rank trajectories; *model training* and *trajectory embedding generation* generate vector representations of trajectories in a multidimensional space; finally *dimensionality reduction* maps the vector representations onto a low-dimensional space.

In summary, the main contributions of our research are: (i) a composite methodology integrating representation learning, advanced trajectory segmentation techniques, and trajectory generalization strategies; (ii) a detailed workflow for the generation of trajectory embeddings; (iii) an evaluation metric for quantifying the goodness of trajectory embeddings; (iv) a validation strategy to assess the similarity of trajectories based on their vector representation.

The *mob2vec* methodology has been tested and evaluated on a dataset of 17000+ CDR trajectories provided by the NPTLab of the University of Milan. The dataset is comparable in size with the datasets used in the Sqn2Vec project.

The rest of the paper is organized as follows: Section 2 provides background knowledge on Sqn2Vec and SeqScan-d techniques; Section 3 introduces the CDR dataset, while Section 4 the *mob2vec* framework; Section 5 and 6 report two different classes of experiments. Section 7 reports some conclusive considerations.

## 2 Background knowledge

In this section, we overview key features of the two major components used in *mob2vec*, i.e. Sqn2Vec and SeqScan-d.

### 2.1 Sqn2Vec

Sqn2Vec [20] is an unsupervised method recently proposed for the learning of symbolic sequence representations and tailored to datasets with relatively small vo-

cabularies. Sqn2Vec builds on Paragraph Vector<sup>1</sup> (PV) [6, 15], and indirectly on word2vec [18], thus is rooted in the representation of variable-length pieces of text and words.

In these algorithms, the real objective of learning a representation of input data is accomplished by trying to solve an auxiliary correlated task. The progress on this task is made by an iterative heuristic procedure that, at the end of each iteration, adjusts the relevant representations using linearly decreasing weights. PV is presented in two variants that differ in the proposed task.

- *Distributed Memory (PV-DM)*. By using the representations of both paragraphs and words, the task is: given a context (i.e. a bunch of consecutive words in a paragraph), predict the next word.
- *Distributed Bag-Of-Words (PV-DBOW)*. By only using the representation of the current paragraph, the task is to predict some of the words of which it is composed. In more detail: at each iteration, a classification task is formed by taking the words in the chosen rolling context as positive samples, and random words drawn from the global word frequency distribution as negative samples. This variant is conceptually simple, requires to store less data and has been demonstrated to be much faster.

PV can be applied not only to plain text, but also on all kinds of symbolic sequences. However, the representation learned by PV is often poor when the training dataset has a small vocabulary. This is typical of CDR datasets, in which users’ trajectories are composed of just a few dozen unique symbols; a more extreme case is the application to DNA sequences, in which the vocabulary size is 4. One of the possible explanations of the poor performance in these cases is that the context surrounding each symbol carries little information; moreover, in these algorithms the context is treated as a set rather than as a sequence, thus losing some information regarding the order in which the symbols appear.

To overcome the above difficulties, Sqn2Vec introduces the following concept: given a threshold  $\delta \in [0, 1]$ , a *sequential pattern satisfying a  $\Delta$ -gap constraint* (SP for short) is a sequence of symbols that occur in at least a fraction  $\delta$  of the dataset sequences; these symbols can have a distance of at most  $\Delta$  each with respect to the following one (see [20] for a formal definition). The idea behind Sqn2Vec is to exploit the property that the size of the SP vocabulary can be – depending on  $\delta$  and  $\Delta$  – several orders of magnitude greater than that of the symbols, so that, by associating to every sequence its set of SPs, it is possible to construct another input dataset for a representation learning algorithm. However, the

<sup>1</sup>Also known as doc2vec after the name of a popular implementation [24].

original sequences cannot simply be replaced by their corresponding set of SPs, because a sequence may not contain any SP; so SPs have to be used *in addition* to the original symbols, and not as a replacement of them.

Sqn2Vec is composed by two phases. The first one is the sequential pattern discovery: fixed a threshold  $\delta$  and a gap  $\Delta$ , a pattern mining procedure computes the set of SPs associated to each original sequence. The second phase of Sqn2Vec is the sequence embedding learning. Both original sequences and their sets of SPs are exploited in this phase, in one of the two following alternative ways.

- *Sqn2Vec-SIM*. For each sequence, its original symbols and its SPs are concatenated and used as input of a single PV-DBOW training process, in which positive and negative samples are drawn from a distribution made of both symbols and SPs.
- *Sqn2Vec-SEP*. The embedding vectors of original sequences and SPs are learned separately in two independent PV-DBOW trainings. The two representation spaces have the same dimensions, so that the resulting vectors can be pairwise averaged at the end of the process, thus producing a unique representation vector for each original sequence. It can be expected that in this variant the training processes will produce more accurate results as they use homogeneous information.

## 2.2 SeqScan-d

SeqScan is a family of density-based trajectory segmentation techniques developed to extract sequences of *relevant* locations (or stay regions) from trajectories, based on a relevance model, and designed to be robust against noise [8].

The outcome of the algorithm is a series of temporally ordered clusters, the *summary trajectory*. Besides, two classes of noise points are identified: (a) the points temporally in between two consecutive clusters, i.e. *transition*. (b) The points representing temporary absences from the cluster, referred to as *local noise* [7]. SeqScan exists in two versions, one for the segmentation of spatial trajectories; the other for the segmentation of discrete, symbolic trajectories taking the form:  $T = (l_1, t_1), \dots, (l_n, t_n)$  where  $l_i$  is a name, or *symbol*, of a dictionary [9]. We refer to the discrete version used in this paper as SeqScan-d. In a symbolic space, a (SeqScan-d) cluster is a segment of maximal length satisfying the model constraints. Such segment can be concisely represented by a unique representative symbol, i.e. the symbol that, based on the model, is *dominant* in the segment period. The algorithm requires two parameters  $N$  and  $\delta$ , the former specifying the minimum number of occurrences for a symbol to be dominant in a segment; the latter the minimum cumulative amount of

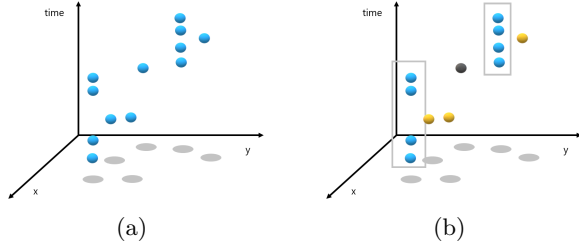


Figure 1: (a) A CDR trajectory with 12 occurrences (in space-time). (b) The rectangles contains two groups of occurrences for the same symbol, i.e. clusters along the temporal line. There are also 3 local noise points (colored in yellow) and one transition point (colored in black) [9].

time that symbol appears in the segment. Summary trajectories can be straightforwardly represented using the symbolic data model in [14]. SeqScan-d has been applied to the summarization of CDR trajectories. Figure 1 exemplifies a CDR trajectory in the discrete spatio-temporal coordinates space.

### 3 The input dataset

We begin describing the CDR dataset used for this work. The dataset is provided by a major mobile operator in Italy. The dataset covers the city of Milan plus a few surrounding districts, over a period of 67 days, from March to May 2012. It contains 17000+ trajectories of anonymized users. The location information is given at the spatial granularity of *Location Area*, where a Location Area is a set of one or more base stations, grouped together by the mobile operator, and univocally identified by a label [9].

Cells and Location Areas coordinates are not available. However, in previous work, it was estimated that 75% of the Location Areas in Milan are smaller than 1 square kilometer and concentrated downtown, whilst the largest regions, over 4 square kilometers, are in the suburbs. Figure 2 shows a fragment of CDR trajectory with in background the Voronoi polygons approximating Location Areas and an example user path. A CDR specifies the user identifier, the timestamp and the Location Area (we omit the communication event, e.g. phone call). The names of the Location Areas form the symbolic space. We refer the reader to [21, 23] for further details on the dataset.

## 4 The *mob2vec* framework

### 4.1 Overview

The *mob2vec* framework supports two tasks: (i) generation of the representation model from the input dataset of CDR trajectories; and (ii) representation *inference* (or

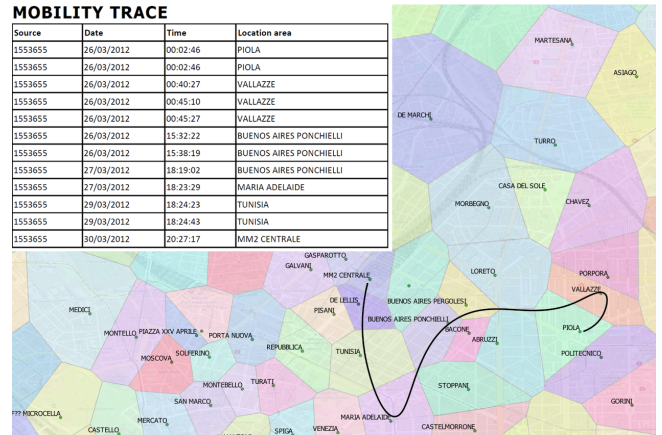


Figure 2: A fragment of CDR trajectory along with the Voronoi diagram approximating the Location Areas.

prediction). The former task is to populate the embedding space with the vector representation of the CDR trajectories of the input dataset; the inference task is to generate the representation of new trajectories, based on the learned model.

The generation of the representation model is the key task comprising four main steps outlined as follows:

- **Data preparation.** Irrelevant and noisy locations are removed from input trajectories using the SeqScan-d technique. The result is a set of summary trajectories. Summary trajectories are generalized into rank trajectories, hence split in smaller units, based on temporal criteria. The result is the *source* dataset.
- **Model training.** Source data are pre-processed to generate the training set for the Sqn2Vec technique. The outcome of this phase is the vector representation of trajectory units.
- **Generation of trajectory embeddings.** The vectors obtained at the previous step are aggregated to form the trajectory embeddings.
- **Dimensionality reduction.** The multimentional embedding space is reduced to a low dimensional space (e.g. 2D space), using the UMAP dimensionality reduction technique [17]. The embedded points in the 2D space represent thus the input CDR trajectories.

The above steps are detailed in the following. The basic notation used throughout the paper is summarized in Table 1.

### 4.2 Data preparation

The input CDR trajectories are processed and a number of transformations are applied to sequential data. The three key operations are:

Table 1: Notation

Symbol	Definition
$T$	CDR trajectory
$T_s$	Summary trajectory
$T_r$	Rank trajectory
$T_w^j$	Weekly (rank) trajectory for week $j$
$t_i$	Timestamp in $T$
$I_i$	Time interval in $T_s, T_r$
$L$	Set of location names / symbolic locations
$R$	Set of frequency rank values
$\text{rk}(l_i), r_i$	Rank of location $i$
$r$	Pearson Correlation Coefficient
$e_i$	embedding

### Trajectory summarization

This operation extracts from every CDR trajectory a sequence of temporally annotated symbols. Each symbol is representative of the series of locations appearing in a trajectory segment compliant with the relevance model of the SeqScan-d technique. Symbols are annotated with the temporal extent of the corresponding segment. The result is a *summary trajectory*:

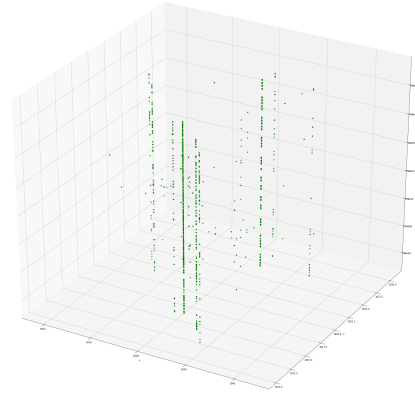
$$T_s = (I_1, l_1), \dots, (I_n, l_n)$$

where the symbolic location  $l_i \in L$  is representative of the  $i$ -th segment detected by the SeqScan-d algorithm, over time interval  $I_i$ . In the rest of the paper, we refer to the locations appearing in summary trajectories as *relevant locations*. Figure 3 shows an example of summary trajectory drawn from the CDR dataset.

The purpose of trajectory summarization is to remove noise and irrelevant locations from native trajectories, which can adversely affect the learning process. Whether a summary trajectory is really representative of the actual movement of an individual is a question that has been tackled in recent work. In [10] we show that summary trajectories preserve major statistical properties of the native CDR trajectories, specifically the distribution of the (location) frequency rank.

### Generation of rank trajectories

Following earlier assumption, the mobility behavior of an individual is independent from the specific locations the user visits. For example, those individuals that mostly frequent home and work exhibit similar behavior, regardless of the actual name of the locations standing for the individual’s home and work. In order to analyze and compare the mobility behavior of users, a more abstract and generalized representation of locations is thus needed. To deal with this issue, we transform symbolic trajectories into *rank trajectories*. Specifically, for every summary trajectory  $T_s$ , we define a mapping  $\text{rk}$  between



(a)

( $l_1$ , TURRO), ( $l_2$ , PALAVOBIS), ( $l_3$ , TURRO), ( $l_4$ , PALAVOBIS),  
 ( $l_5$ , GALLARATESE), ( $l_6$ , TURRO), ( $l_7$ , PALAVOBIS), ( $l_8$ , GALLARATESE),  
 ( $l_9$ , TURRO), ( $l_{10}$ , PALAVOBIS), ( $l_{11}$ , TURRO), ( $l_{12}$ , PALAVOBIS),  
 ( $l_{13}$ , LAMPUGNANO), ( $l_{14}$ , PALAVOBIS), ( $l_{15}$ , TURRO),

....

\*  $l_1 = [2012-03-26\ 08:22:40, 2012-03-26\ 17:10:55]$ ,

$l_2 = [2012-03-26\ 18:07:17, 2012-03-27\ 00:00:00], \dots$

(b)

Figure 3: CDR trajectory #1472043. (a) Graphical representation in a spatio-temporal coordinate system. The points in the plane are the Location Area centroids. (b) Portion of the corresponding summary trajectory.

the locations appearing in  $T_s$  and the set of frequency ranks  $R = \{1, 2, \dots, r_{\max}\}$ . The ranking is drawn from the number of times relevant locations appear in the trajectory. If multiple locations have the same frequency, we assign them increasing rank values, so that  $\text{rk}$  is a bijective function. By replacing the symbolic location  $l_i$  with the corresponding rank  $\text{rk}(l_i)$ , we obtain the rank trajectory:

$$T_r = (I_1, r_1), \dots, (I_n, r_n)$$

with  $r_i \in R$ . Location names are thus replaced by symbols representing ordinal values. Rank trajectories share a common set of symbols, in particular the lowest ranks. Therefore, the size of the vocabulary is significantly smaller than the original location dictionary.

**Example 1.** Rank trajectory for id=1472043: for brevity, we omit the temporal information and only report the series of ordinal values (delimited by square brackets):

$T = [2\ 1\ 2\ 1\ 4\ 2\ 1\ 4\ 2\ 1\ 2\ 1\ 5\ 1\ 2\ 1\ 2\ 8\ 1\ 2\ 1\ 7$   
 $1\ 2\ 1\ 2\ 1\ 9\ 1\ 3\ 1\ 2\ 1\ 2\ 1\ 2\ 1\ 3\ 1\ 11\ 2$   
 $1\ 2\ 1\ 2\ 1\ 2\ 1\ 2\ 1\ 2\ 1\ 2\ 10\ 1\ 2\ 1\ 2\ 1\ 2$

1 5 1 2 1 2 12 1 2 3 1 2 1 2 1 2 1 2 1 2 1  
 2 1 2 1 2 1 2 6 1 2 1 2 1 2 1]

The value  $k$  represents the  $k$ -th most frequented location in the trajectory. For example, the location of rank 1 is also referred to in literature as *home*, the location of rank 2 as *work*.

### Trajectory splitting

This operation takes into account the temporal dimension of trajectories. To begin, the observation period is slightly shortened so as to cover an exact number of weeks (a week covers the period from Monday to Sunday). Rank trajectories are thus split in smaller trajectories, one per week. Therefore, for any trajectory  $T_r$ , we obtain a set of *weekly trajectories*  $T_w^1, \dots, T_w^m$ , with  $m$  the number of weeks. The split rule is as follows. For every value  $r_i$  in  $T_r$  consider the period  $I_i$ . If the starting time of  $I_i$  falls into week  $j \in \{1, \dots, m\}$ ,  $r_i$  is assigned to  $T_w^j$ . Weekly trajectories are only defined at symbolic level, while timestamps are ignored, i.e.

$$T_w^j = (r_1, \dots, r_k).$$

**Example 2.** The above trajectory is split in a series of 10 weekly trajectories  $T_w^1, \dots, T_w^{10}$ .

[2 1 2 1 4 2 1 4 2 1 2 1 5 1]  
 [2 1 2 8 1 2 1 7]  
 [1 2 1 2 1 9 1 3 1]  
 [2 1 2 1 2 1 2 1 3 1 11]  
 [2 1 2 1 2 1 2 1]  
 [2 1 2 1 2 1 2 10 1]  
 [2 1 2 1 2 1 5 1 2 1]  
 [2 12 1 2 3 1 2 1 2 1 2 1]  
 [2 1 2 1 2 1 2 1 2 1]  
 [2 6 1 2 1 2 1 2 1]

A certain regularity can be noticed in the weekly movement, in line with what is reported in literature.  $\diamond$

### 4.3 Model training

Weekly trajectories are encoded in the form requested by the Sqn2Vec technique. The Sqn2Vec architecture consists of two feedforward neural networks that are to be trained separately. One of these networks is trained with the weekly trajectories obtained at the previous step; the second network with the sequential patterns appearing more frequently in the whole dataset given a support threshold and a symbol gap tolerance. Sequential patterns are defined at dataset scale. Both symbols and sequential patterns are indexed based on two distinct vocabularies. Hence, for every weekly trajectory, we have two one-hot vectors, one for each training set.

The following example illustrates the indexing of sequential patterns.

**Example 3.** The sets of sequential patterns extracted from the weekly trajectories in Example 2 are:

SP1={1 5 7 9 65 186 255 259 262 337}  
 SP2={1 7 8 13 65 66 255 266 312}  
 SP3={1 6 7 17 65 221 255 260 270 582}  
 SP4={1 6 7 10 65 221 255 260 263}  
 SP5={1 7 65 255}  
 SP6={1 7 24 65 82 255 762}  
 SP7={1 5 7 65 186 255 259}  
 SP8={1 6 7 11 64 65 69 221 255 410}  
 SP9={1 7 65 255}  
 SP10={1 7 12 65 70 255 439}

Every index corresponds to a sequential pattern appearing frequently in the dataset. For example, index 255 corresponds to the two-symbol pattern (1,2), whilst 259 to (1,5).  $\diamond$

Once the input data is organized, the training of the model is performed using the architecture Sqn2Vec-SEP. Sqn2Vec-SEP assigns each trajectory of the two datasets an incremental identifier (the correspondent of the document identifier) and then applies the PV-DBOW technique to train the two models. As a result, for each weekly trajectory  $i$ , we obtain two vector representations in a multi-dimensional embedding space (128 dimensions),  $\mathbf{v}_1^{(i)}$  and  $\mathbf{v}_2^{(i)}$ . The average vector:

$$\mathbf{v}^{(i)} = \frac{\mathbf{v}_1^{(i)} + \mathbf{v}_2^{(i)}}{2}$$

is the final representation of the weekly trajectory  $i$ , the *weekly embedding*.

### 4.4 Generating trajectory embeddings

The next step is to scale up the trajectory representation from weekly to full trajectories. Full trajectories cover the whole observation period and are univocally associated to users. To motivate this operation, consider Figure 4.

This figure shows the plot of a small set of weekly embeddings in the two dimensional space obtained by applying the popular t-SNE dimensionality reduction technique. Every point in space represents a weekly trajectory, while the color of the point the full trajectory identifier, i.e. the user. It can be seen that points are clustered by color, namely the weekly trajectories of every user are mapped onto points that are close in space. This is an interesting result, surprisingly in line with the literature on human mobility, according to which the mobility behavior of an individual is similar across the weeks. Motivated by this empiric observation, we



Table 2: Datasets used in experiments

Dataset	Description
$D_0$	Native dataset of 17000+ CDR trajectories
$D_1$	Dataset of summary trajectories drawn from $D_0$ , by running SeqScan-d with parameters $N = 4, \delta = 15'$
$D_2$	Dataset of weekly trajectories, i.e. summary trajectories ( $D_1$ ) split in weeks
$D_3$	Dataset of rank trajectories drawn from summary trajectories ( $D_1$ )
$D_4$	Dataset of rank trajectories drawn from weekly trajectories ( $D_2$ )
$D_5$	Dataset of rank trajectories drawn from $D_0$ (no summarization) split in weeks

Table 3: Summary statistics for the datasets used for *mob2vec* evaluation

Dataset	Trajectories	Symbols	Max. length	Avg. length
$D_0$	17241	233	510	107.18
$D_1$	151107	233	78	12.22
$D_2$	17241	95	510	107.18
$D_3$	151107	95	78	12.22
$D_4$	152739	242	12133	316.42
$D_5$	1010238	108	88	9.42

**Hardware and software settings.** For the experiments we have used the following settings. Hardware: HP ProLiant ML350 G6, with Windows 10 LTSC 1809, equipped with: CPU Intel Xeon X5675 6core/12threads, 120GB DDRIII ECC RAM, 500GB SSD. Relevant software libraries and platforms: PostGIS; PyCharm 2019; scikit-learn 0.22.1; umap-learn 0.3.10; gensim 3.8.0; github.com/nphdang/Sqn2Vec post commit 056cc53 (Sqn2Vec).

## 5.2 Evaluation metric

Consider two rank trajectories  $T_1, T_2$ . We define:

- The distance between the corresponding trajectory embeddings  $e_1, e_2$  is the Euclidean distance  $d(e_1, e_2)$  on the 2D plane.
- The distance between the probability distributions  $g_1, g_2$  of the rank symbols is the Jensen-Shannon distance  $D_{JS}(g_1, g_2)$ , i.e. the square root of the Jensen-Shannon divergence [12].  $D_{JS}$  is based on the KullbackLeibler divergence ( $D_{KL}$ ) and have some useful properties: in particular, is a metric and takes values ranging between 0 and 1.  $D_{JS}$  is defined as

Table 4: Summary statistics for the datasets used for Sqn2Vec evaluation

Dataset	Sequences	Symbols	Max. length	Avg. length
reuters	1010	6380	533	93.84
aslbv	424	250	54	13.05
aslgt	3464	94	176	43.67
auslan2	200	16	18	5.53
context	240	94	246	88.39
pioneer	160	178	100	40.14
skating	530	82	240	48.12
unix	5472	1697	1400	32.34
average	1437	1099	346	45.64

follows:

$$D_{JS}(g_1, g_2) = \sqrt{\frac{1}{2}D_{KL}(g_1|M) + \frac{1}{2}D_{KL}(g_2|M)}$$

where  $M = \frac{1}{2}(g_1 + g_2)$ .

Given a dataset of rank trajectories, we compute for every pair of trajectories  $i, j$ , the point of coordinates  $d(e_i, e_j)$  and  $D_{JS}(g_i, g_j)$ , respectively, hence the linear correlation between the two distances using the Pearson linear correlation coefficient  $r \in [-1, +1]$ . The evidence of a strong positive correlation (i.e.  $0.5 \leq r \leq 1$ ) is interpreted as goodness of the trajectory embeddings (based on the given hypothesis).

## 5.3 Experiment 1: dimensionality reduction

The goal is to evaluate to what extent the dimensional reduction of the trajectory embeddings is beneficial for the learning process. The method is as follows. We start evaluating the goodness of embeddings when the space dimensions are not reduced, next we analyze various options for the reduction of dimensionality. The source dataset is  $D_4$ , i.e. rank trajectories split in weeks. The dimension of the trajectory embeddings is set to 128. The experiments are:

**Exp. 1.1** For generality, we consider two distance functions in the embedding space, the cosine similarity and the Euclidean distance. Table 5 reports the coefficient  $r$  resulting in the two cases. It can be seen that there is no evidence of strong linear correlation.

Table 5: No dimensionality reduction

Space dimensions	Distance	$r$
128	cosine	0.0508
128	Euclidean	0.3628

**Exp. 1.2** Seven dimensionality reduction techniques have been selected for evaluation and comparison. Specifically:

- Principal Component Analysis (PCA);
- Isometric Mapping (IsoMap);
- Multi-dimensional Scaling (MDS);
- t-distributed Stochastic Neighbor Embedding (t-SNE);
- Locally Linear Embedding (LLE);
- Spectral Embedding;
- Uniform Manifold Approximation and Projection for Dimension Reduction (UMAP).

The evaluation considers both the coefficient  $r$  and the computational efficiency of the technique (run time). The results are computed by extracting the vectors at the end of the training. They are shown in Table 6, while a few exemplifying plots are reported in Figure 5. It can be seen that PCA and UMAP are the most efficient and also the value of  $r$  is high, i.e. the trajectory embeddings are coherent with symbol distribution. Unlike PCA, and in the same line of t-SNE applied for visualization purposes in [20], UMAP is a non-linear transformation technique. UMAP is chosen as part of the methodology and used in the rest of the experiments. Figure 6 illustrates the meaning of the linear correlation coefficient computed for UMAP.

Table 6: Evaluation of dimensional reduction techniques

Technique	$r$	Runtime [s]
PCA	0.7100	1
IsoMap	0.6376	433
MDS	0.5075	1696
t-SNE	0.6487	277
LLE	0.6285	529
Spectral	0.5493	473
UMAP	0.7302	69

#### 5.4 Experiment 2: space dimensions

We evaluate the impact of the embedding space dimension over the correlation  $r$ . A strong correlation  $r$  can be observed in higher dimensional spaces. Table 7 reports the value of  $r$  for spaces of 64, 128 and 256 dimensions, respectively. As in Sqn2Vec, we choose an embedding space of 128 dimensions.

#### 5.5 Experiment 3: PV-DM vs. PV-DBOW

The Sqn2Vec technique relies on the architecture PV-DBOW, which in [20] is proven more effective than PV-DM. We recall that PV-DM is the context-aware neural

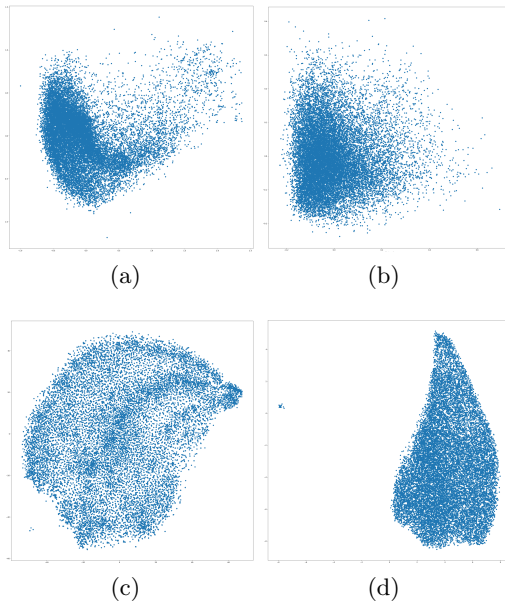


Figure 5: Examples of dimensional reduction of trajectory embeddings: (a) Isometric Mapping; (b) Principal Component Analysis; (c) t-SNE; (d) UMAP. In all non-linear methods (a, c, d) the axes have no specific meaning: any rotation produces an equally valid embedding.

Table 7: Impact of the number of dimensions

Space dimensions	$r$
64	0.7224
128	0.7302
256	0.7176

network architecture defined in [15]. In this experiment, we evaluate whether we can reach the same conclusion using our evaluation metric for comparison. We also compare the efficiency of the training process. The parameter indicating the width of the context window (PV-DM) is set to 5 symbols. Results are reported in Table 8. It is shown that PV-DBOW has a better performance, in line with the literature. The evaluation metric is coherent.

Table 8: Experiment 3: PV-DBOW vs. PV-DM

NN Architecture	$r$	Training duration [s]
PV-DM	0.5704	22412
PV-DBOW	0.7302	9802

#### 5.6 Experiment 4: location vs. rank

A key step of the learning process is the generalization of summary trajectories into learning rank trajectory-

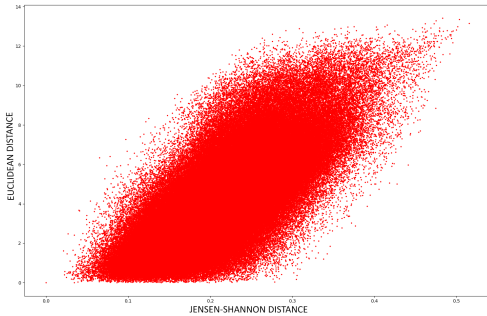


Figure 6: Scatter plot of points representing pairs of rank trajectories: the y-axis reports the Euclidean distance of the embeddings computed with UMAP, the x-axis the Jensen-Shannon distance between symbol distributions

ries. In this experiment, we consider two different source datasets, i.e.  $D_2$  and  $D_4$ , containing summary and rank trajectories respectively. Two sets of trajectory embeddings are then generated and finally evaluated using the  $r$  coefficient. Table 9 reports the results. It is evident that rank trajectories are key for the learning of behavioral models.

Table 9: Experiment 4: location vs. rank symbols

Trajectory type	$r$
Summary trajectories ( $D_2$ )	0.0036
Rank trajectories ( $D_4$ )	0.7302

### 5.7 Experiment 5: native vs. summary data

Summary trajectories contain *relevant* locations extracted from native trajectories using the SeqScan-d technique. The main purpose of this operation, called summarization, is to remove noise and insignificant locations. In this experiment, we evaluate the impact of summarization. We consider the dataset  $D_5$  of native trajectories and the data set  $D_4$  of summary trajectories, and evaluate the coefficient  $r$  in two embedding spaces, of 128 and 256 dimensions, respectively. Table 10 reports the evaluation. It can be seen that the coefficient  $r$  and thus the quality of embeddings is definitely higher when summary trajectories are used.

## 6 Experiments: behavioral similarity

We turn to evaluate the capability of preserving behavioral similarity. The goal is to create trajectories similar to those defined in the training set, and then evaluate the distance among the respective embeddings. Following the methodology, we should find that those embeddings are in proximity. The first non-trivial question is how to specify trajectories, and more specifically

Table 10: Experiment 5: native vs. summary trajectories

Trajectory type	Space dimensions	$r$
Native trajectories ( $D_5$ )	128	0.0615
Summary trajectories ( $D_4$ )	128	0.7302
Native trajectories ( $D_5$ )	256	0.0348
Summary trajectories ( $D_4$ )	256	0.7176

rank trajectories, that are *similar* to those of the training set. To tackle the problem, an approach [16] is to apply down-sampling and distortion. In that project, however, trajectories are spatial trajectories acquired at high sampling rate, while rank trajectories are sequences of ordinal values corresponding to sparse locations. We thus propose a different approach. The idea is to remove from the rank trajectories the values occurring in the sequence that are less significant because they correspond to locations that are rarely frequented (i.e. the ranks of higher value). It can be seen that the removal of the rank value  $n$  from a trajectory does not alter the lowest ranks  $1, 2, \dots, n-1$ , that is, the relevant characteristics of the mobility behavior of an individual are not altered. In this sense, this form of down-sampling generates rank trajectories that are slightly different from the original trajectories and thus are *similar*. The experiment is as follows. We randomly select 1000 trajectories from the source dataset  $D_4$  (source trajectories). For every trajectory, we create 5 *similar* trajectories by removing the  $k$  less significant rank values for  $k \in [1, 5]$ . The degree of similarity thus decreases for increasing values of  $k$ . Based on these data, we use the functionality of representation inference to generate the embeddings for the similar trajectories. The boxplot in Figure 7 describes the variation in distance between similar trajectories and source trajectories for increasing value of  $k$ . The red line in the figure reports the maximum distance between two embedded points. It can be seen that: (a) the distance measures are relatively small; (b) on average, the distance increases monotonically with the value of  $k$ . These results are coherent with the methodological framework.

Visual evidence of the previous result is given in Figure 8. In particular, the figure highlights the representation of a specific trajectory in the 2D embedding space (point with index 0), close to the embedded points of the five similar trajectories (indices 1 to 5).

Further insights are provided by Figure 9. The figure highlights the embedded points representing the four summary trajectories displayed in the spatio-temporal coordinated space. In this case the trajectories belong to the source dataset  $D_4$ . It can be seen that the distance reflects the diversity of the trajectories. In particular the furthest point represents a trajectory that appears

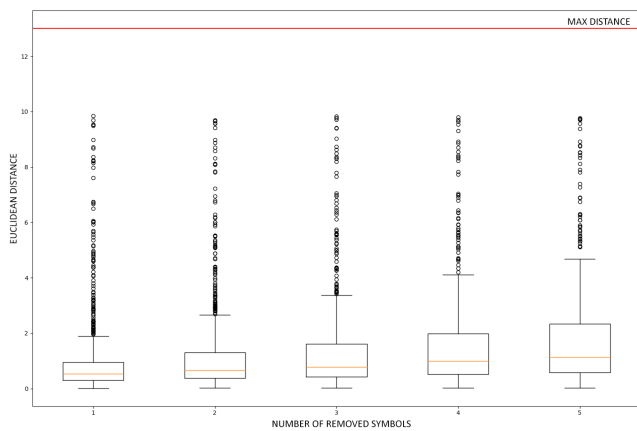


Figure 7: Boxplot reporting the distribution of the Euclidean distance between the embeddings of source trajectories and similar trajectories for increasing values of removed ranks.

substantially different from the other trajectories.

## 7 Conclusions

In this paper, we have presented the *mob2vec* framework for mapping CDR trajectories into vector representations capable of preserving mobility behavior similarity. The approach builds on Sqn2Vec for the learning of sequence representations. Yet, Sqn2Vec does not provide any support for time, neither for noisy data and behavioral similarity, which instead is the major contribution of this work. We have been able to show the effectiveness of key choices: the generalization of movement in rank trajectories; noise removal; the aggregation of temporally-bounded vectors; the evaluation of the embedding quality; the UMAP dimensionality reduction of the embedding space. The result is exciting. We plan to apply the technique to other datasets, in order to consolidate the results. Yet, the major challenge is to provide a theoretical explanation, corroborating the empirical achievements.

**Acknowledgments** The research carried out by M. L. Damiani, F. Hachem and M. Rossini is partially supported by the Italian government via the NG-UWB project (MIUR PRIN 2017).

## References

- [1] H. Barbosa, M. Barthelemy, G. Ghoshal, C. R. James, M. Lenormand, T. Louail, R. Menezes, J. J. Ramasco, F. Simini, and M. Tomasini. Human mobility: Models and applications. *Physics Reports*, 734:1 – 74, 2018.
- [2] Y. Bengio, A. Courville, and P. Vincent. Representation learning: A review and new perspectives. *IEEE Transactions on Pattern Analysis and Machine Intelligence*, 35(8):1798–1828, 2013.

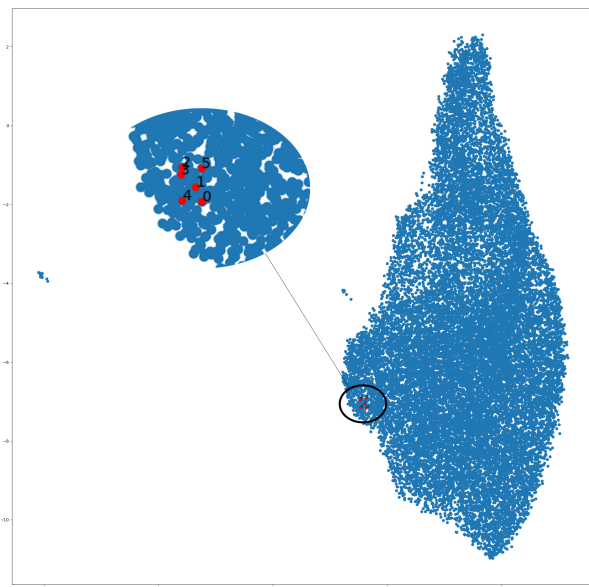


Figure 8: Visual analysis of embeddings: source trajectory (point 0) and the five similar trajectories (points 1 to 5).

- [3] K. Bringman and M. Künnemann. Multivariate fine-grained complexity of longest common subsequence. In *Proc. of the 29th ACM-SIAM Symposium on Discrete Algorithms*, pages 1216–1235, 2018.
- [4] D. K. Chandra, P. Wang, J. Leopold, and Y. Fu. Collective representation learning on spatiotemporal heterogeneous information networks. In *Proc. of the 27th ACM SIGSPATIAL*, 2019.
- [5] B. Csaji, A. Browet, V. Traag, J. Delvenne, E. Huens, P. Van Dooren, Z. Smoreda, and V. D. Blondel. Exploring the mobility of mobile phone users. *Physica A: Statistical Mechanics and its Applications*, 392(6):1459 – 1473, 2013.
- [6] A. M. Dai, C. Olah, and Q. Le. Document embedding with paragraph vectors. *arXiv preprint arXiv:1507.07998*, 2015.
- [7] M. L. Damiani and F. Hachem. Segmentation techniques for the summarization of individual mobility data. *Wiley Interdisciplinary Reviews: Data Mining and Knowledge Discovery*, 7(6), 2017.
- [8] M. L. Damiani, F. Hachem, H. Issa, N. Ranc, P. Moorcroft, and F. Cagnacci. Cluster-based trajectory segmentation with local noise. *Data Mining and Knowledge Discovery*, 32(4):1017–1055, 2018.
- [9] M. L. Damiani, F. Hachem, C. Quadri, and S. Gaito. Location relevance and diversity in symbolic trajectories with application to telco data. In *Proc. of the 16th International Symposium on Spatial and Temporal Databases, SSTD*, pages 41–50, 2019.
- [10] M. L. Damiani, F. Hachem, C. Quadri, M. Rossini, and S. Gaito. On location relevance and diversity in human mobility data. *ACM TSAS*, In press.

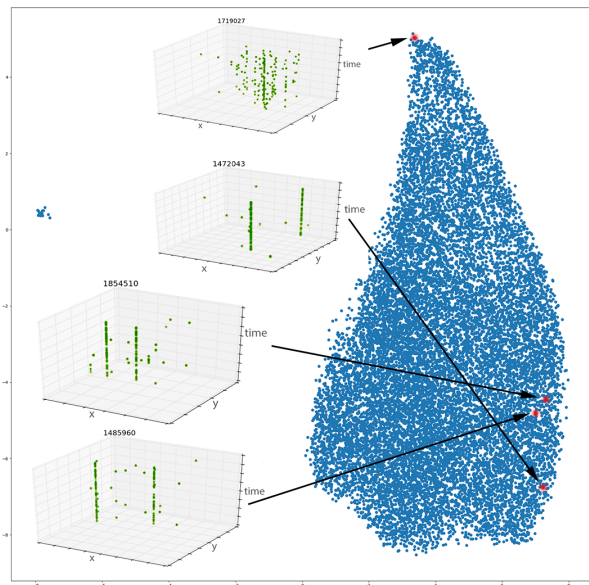


Figure 9: The embeddings corresponding to the four trajectories represented in the spatio-temporal space.

- [11] P. Fournier-Viger, J. C.-W. Lin, R. U. Kiran, Y.-S. Koh, and R. Thomas. A survey of sequential pattern mining. *Data Science and Pattern Recognition*, 1(1):54–77, 2017.
- [12] B. Fuglede and F. Topsoe. Jensen-Shannon divergence and Hilbert space embedding. In *Proc. of the IEEE International Symposium on Information Theory*, 2004.
- [13] M. C. Gonzales, C. Hidalgo, and A. Barabasi. Understanding individual human mobility patterns. *Nature*, 453(7196):779–782, 2008.
- [14] R. H. Güting, F. Valdés, and M. L. Damiani. Symbolic trajectories. *Trans. Spatial Algorithms and Systems*, 1(2):7:1–7:51, 2015.
- [15] Q. Le and T. Mikolov. Distributed representations of sentences and documents. In *Proc. of the 31st International Conference on Machine Learning (ICML)*, volume 32, page III188III196. JMLR.org, 2014.
- [16] X. Li, K. Zhao, G. Cong, C. S. Jensen, and W. Wei. Deep representation learning for trajectory similarity computation. In *Proc. of IEEE 34th International Conference on Data Engineering (ICDE)*, 2018.
- [17] L. McInnes, J. Healy, and J. Melville. Umap: Uniform manifold approximation and projection for dimension reduction. *arXiv preprint arXiv:1802.03426*, 2018.
- [18] T. Mikolov, I. Sutskever, K. Chen, and J. Dean. Distributed representations of words and phrases and their compositionality. In *Advances in Neural Information Processing Systems 26*. 2013.
- [19] C. Mooney and J. Roddick. Sequential pattern mining—approaches and algorithms. *ACM Computing Surveys (CSUR)*, 45(2):1–39, 2013.
- [20] D. Nguyen, W. Luo, T.-D. Nguyen, S. Venkatesh, and D. Phung. Sqn2Vec: Learning sequence representation via sequential patterns with a gap constraint. In *Machine Learning and Knowledge Discovery in Databases*, pages 569–584. Springer International Publishing, 2019.
- [21] M. Papandrea, K. Keramat, M. Zignani, S. Gaito, S. Giordano, and G. Rossi. On the properties of human mobility. *Computer Communications*, 87:19–36, 2016.
- [22] L. Pappalardo, F. Simini, S. Rinzivillo, D. Pedreschi, F. Giannotti, and A. Barabási. Returners and explorers dichotomy in human mobility. *Nature communications*, 6(1):1–8, 2015.
- [23] C. Quadri, M. Zignani, S. Gaito, and G. P. Rossi. On non-routine places in urban human mobility. In *Proc. of IEEE 5th International Conference on Data Science and Advanced Analytics (DSAA)*, 2018.
- [24] R. Řehůřek and P. Sojka. Software framework for topic modelling with large corpora. In *Proc. of the LREC Workshop on New Challenges for NLP Frameworks*, pages 45–50. ELRA, 2010.
- [25] C. Song, T. Koren, P. Wang, and A. Barabasi. Modelling the scaling properties of human mobility. *Nature Physics*, 6:818823, 2010.
- [26] S. Taghizadeh, A. Elekes, M. Schler, and K. Bhm. How meaningful are similarities in deep trajectory representations? *Information Systems - in press*, 2019.
- [27] P. Wang, Y. Fu, H. Xiong, and X. Li. Adversarial sub-structured representation learning for mobile user profiling. In *Proc. of ACM SIGKDD (KDD’19)*, 2019.
- [28] P. Wang, Y. Fu, J. Zhang, P. Wang, Y. Zheng, and C. Aggarwal. You are how you drive: Peer and temporal-aware representation learning for driving behavior analysis. In *Proc. of ACM SIGKDD (KDD’18)*, 2018.
- [29] B. Yan, K. Janowicz, G. Mai, and S. Gao. From itdl to place2vec: Reasoning about place type similarity and relatedness by learning embeddings from augmented spatial contexts. In *Proc. of the 25th ACM SIGSPATIAL*, 2017.